

Aircraft atypical approach detection using functional principal component analysis

Gabriel Jarry, Daniel Delahaye, Florence Nicol, Eric Féron

▶ **To cite this version:**

Gabriel Jarry, Daniel Delahaye, Florence Nicol, Eric Féron. Aircraft atypical approach detection using functional principal component analysis. Journal of Air Transport Management, 2020, 84, pp.101787. 10.1016/j.jairtraman.2020.101787 . hal-02506305

HAL Id: hal-02506305

https://enac.hal.science/hal-02506305

Submitted on 13 Mar 2020

HAL is a multi-disciplinary open access archive for the deposit and dissemination of scientific research documents, whether they are published or not. The documents may come from teaching and research institutions in France or abroad, or from public or private research centers.

L'archive ouverte pluridisciplinaire **HAL**, est destinée au dépôt et à la diffusion de documents scientifiques de niveau recherche, publiés ou non, émanant des établissements d'enseignement et de recherche français ou étrangers, des laboratoires publics ou privés.

Aircraft Atypical Approach Detection using Functional Principal Component Analysis

Gabriel Jarry, Daniel Delahaye, Florence Nicol
ENAC, Université de Toulouse, France
Toulouse, France
Email: {gabriel.jarry, daniel.delahaye, florence.nicol}@enac.fr
Eric Feron
King Abdullah University of Science and Technology
Division of Electrical, Computer and Mathematical Science and Engineering
on leave from Georgia Institute of Technology,
Thuwal, 23955, Saudi Arabia
Email: eric.feron@kaust.edu.sa

***Abstract*—In this paper, a post-operational detection method based on functional principal component analysis and clustering is presented and compared with regard to designed operational criteria. The methodology computes an atypical scoring on a sliding window. It enables not only to detect but also to localize where trajectories deviate statistically from the others. The algorithm is applied to the total energy management, estimated from ground-based data, during approach and landing. The detected atypical flights show non-nominal energy behaviors such as glide interceptions from above or high speed approaches. This promising methodology could help to enhance flight data analysis and safety, highlighting non-monitored behaviors.**

***Index Terms*—Approach Path Management, Atypical Flight Event, Non-Compliant Approach, Functional Principal Component Analysis, Unsupervised Learning, Anomaly Detection**

GLOSSARY

ATC Air Traffic Control. 2

CDG Charles De Gaulle Airport. 2, 6, 7, 9

FDA Functional Data Analysis. 2–4
FPCA Functional Principal Component Analysis. 2–5, 7–9

GIFA Glide Interception From Above. 2, 5, 7, 9

NCA Non-Compliant Approach. 1, 2, 5
NSA Non-Stabilized Approach. 1

I. INTRODUCTION

A. Operational Motivations

Approach and landing accidents (i.e. accidents that occur during the initial approach, the intermediate approach and during landing) represent every year 47% of the total number of accidents, and 40% of fatalities [1]. Moreover, a large majority of accidents presents significant differences from nominal approaches such as atypical speed or atypical altitude [2]. In addition, Airport Terminal Maneuvering Areas and Control Traffic Regions are characterized by a dense air traffic flow of high complexity. This complexity will surely increase since IATA forecast growth in air passengers worldwide from around 4 billion today, up to 7.8 billion in 2036 [3]. Consequently, there is a crucial need for aircraft atypical approach detection.

To respond to International Civil Aviation Organization safety requirements, the French Civil Aviation Authority has launched since 2006 a national safety program, which for the time being, is divided into three State Safety Programs published for the period 2009-2013 [4], 2013-2018 [5] and 2018-2023 [6]. The risk portfolio [7] distinguishes undesirable events such as Non-Stabilized Approaches (NSA), from ultimate events such as control flights into terrain, or mid-air collisions. Undesirable events may lead to final events and therefore jeopardize safety or reduce airfield capacity. Their identification and detection is an important issue.

In nominal operations, flight path safety management consists in procedures which guide the aircraft to intercept the extended runway centre line, and the runway slope with an expected configuration in order to land. A particular undesirable event called Non-Compliant Approaches (NCA) was defined in the second version of the 2008-2013 safety program risk portfolio [7]. An approach is considered not compliant when the intermediate and the final leg intercepting conditions do not comply with the prescription of the operational documentation. It may occur during either vectored or non-vectored approaches, and for visual or instrument approaches. An NCA is a potential precursor of NSA [8]. A stabilized approach is one in which the pilot establishes and maintains a constant angle glide-path, an approach speed and an aircraft configuration towards a predetermined point on the landing runway.

Geometrical criteria with horizontal and lateral margins from the nominal path were defined to distinguish a compliant from a non-compliant approach. In particular, interception chevrons were created. They define a 45° maximum angle of procedure radial interception. This angle may be reduced to 30° in specific situations such as dependent parallel runways. Besides, a flight is expected to attend a 30-second levelled off flight during the intermediate leg before descending on runway slope in order to reduce speed and to configure properly for

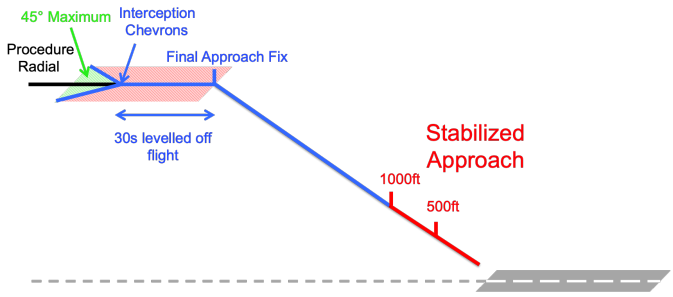


Figure 1. This figure describes Compliant Approach Criteria and illustrates Stabilized Approaches.

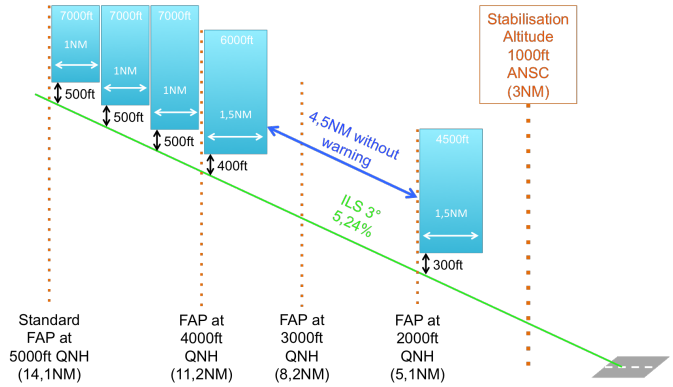


Figure 2. Illustration of Area Proximity Warning set up at CDG airport.

landing. Figure 1 illustrates these criteria.

Non-Stabilized Approaches were found in several accidents such as the Air Nostrum flight 8313 on July, 30th 2011, where the aircraft suffered structural damage following a hard landing at Barcelona Airport [9]. Peeks of descent rate above 3000ft/min were recorded and the aircraft flew over the runway threshold at 315ft, where nominal Reference Datum Height (RDH), i.e. the nominal height above threshold on-glide is around 50ft. Another example is the crash of Asiana Airline flight 214 of July, 6th 2014 at San Francisco Airport, which counted 3 fatalities and 185 injuries [10]. The airplane was recorded with a very low speed in the final approach and finally stalled before crashing.

B. Previous Related Works in ATC

Compliance criteria were applied to flight operations to give an overview of the current situation at Paris Charles-De-Gaulle (CDG) Airport between February and August 2014. The NCA module of the French Civil Aviation Authority tool called ELVIRA was used. This module is a post-operational analysis tool that studies radar trajectories and describes their compliance. Over this period, 22% of flights were detected as non-compliant with approximately 2% being significant. It implies that the definition of compliance could be improved since a large majority of detected non-compliant flights, do not present significant safety issues. Too many false non-compliant alarms may occur, which is troublesome for Air Traffic Control (ATC) operations. Besides, a lack of energy features was underlined. This study led to the identification of different contributing factors and bias for NCAs such as extra energy owing to high speed or tailwind in the final approach, or the influence of QNH during the operations. Specific atypical situations called Glide Interception From Above (GIFA) were pointed out. These situations are particularly critical owing to the potential difficulties to manage aircraft energy and because aircraft are neither designed nor certified to intercept the glide slope from above.

To improve safety and decrease the number of GIFA, an online detection tool was set up at CDG Airport and used by ATCs in real-time. It is composed of four 3D-volumes using the Area Proximity Warning (APW) described in Figure 2. The first three volumes are warning volumes, the ATCs advise pilots that they are too high on glide. The final volume is a decision volume, where ATC and pilots must decide to continue or to interrupt the approach.

The results of the experiments are positive since today GIFAs are detected and an appropriate measure is taken. Approximately 5 flights of the 700 per day raise an alarm and in about half of the cases, ATCs suggest a recovery slope as recommended.

This paper presents new criteria that extend those defined in the NCA module of ELVIRA and defines off-line methodologies based on the specific total energy of the aircraft and Functional Principal Component Analysis.

C. Functional Data Analysis Approach

Functional Principal Component Analysis (FPCA), is a powerful mathematical tool from Functional Data Analysis (FDA). FDA consists in studying a sample of random functions generated from an underlying random variable [11]. They significantly evolved during the 2000s with Ramsay et Silverman [11]–[13]. Other theoretical and applied aspects aspects such as regression or clustering were published by Ferraty and Vieu [14], [15]. In practise, FPCA provides a simple, consistent, and practical representation of high dimensional functional objects such as trajectories, taking into consideration the values and the variation of these functions. In all cases, a prepossessing such as a re-sampling would be necessary before going through unsupervised learning process. The FPCA also provides a solution to dimensionality curse [16] by reducing the dimension. Consequently, it is known to be efficient on time series like trajectories, and motivates its use in this paper.

The applications of FDA are numerous. In [17] Ullah et al. state many applications and underline its multidisciplinary purpose. In particular, FDA is used in various research fields such as medicine, biomedical, biology, finance and demography. In aeronautics, FDA is also widespread. Gregorutti [18] uses data from flight data recorders to develop a prediction tool for long and hard landings. The tool mixes FDA and wavelet decomposition with machine learning such as random forests. During his Ph.D., a software was developed and is now commercialized by a company called SafetyLine. Suyundikov [19] presented a multivariate functional data clustering from trajectories using FPCA in Sobolev spaces. Sobolev spaces are

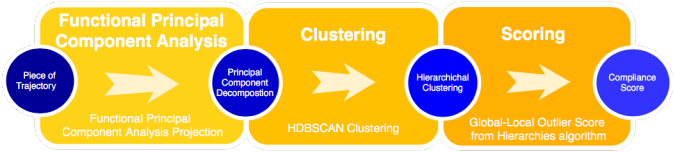


Figure 3. Illustration of the underlying process on each window slide

particular mathematical spaces that naturally ensure smoothness and are therefore usually chosen to represent aircraft trajectories. Hurter et al. [20] developed a bundling algorithm for radar trajectory visualization based on a smoothing spline decomposition and FPCA. Tastambekov [21] developed an aircraft trajectory predictor based on local functional regression with wavelet decomposition and a k-means clustering algorithm. Nicol [22] applied FPCA to study the underlying variation mode of aircraft trajectories. Barreyre et al. presented a novel outlier detection tool in functional data [23], and a statistical outlier detection [24] for space telemetries, based on wavelet decomposition and principal component analysis. Finally, Yan et al. [25] proposed to apply FPCA to a sliding window for dynamic prediction of longitudinal biomarker data, in order to enhance performance robustness.

The contribution of this paper is a novel method using FPCA to detect atypical behaviors applied to aircraft energy management during approach. The innovative paradigm taken in this methodology is to consider atypical, a trajectory that does not follow in terms of values and variations the group behavior. In addition, the use of a sliding window is a major contribution that enables a localization of the atypical behaviors.

The developed method consists in applying the following process recursively, on a sliding window and to the whole data-set. First, the dimension is reduced using the FPCA process on the total energy trajectories. Next, an atypical coefficient scoring is computed using hierarchical clustering and outlier scoring. Finally, all the windows are aggregated together. The underlying process on each window slide is illustrated in Figure 3. Trajectories with an atypical atypical coefficient above a threshold value during a reference duration are considered as atypical.

The paper is divided into four parts. Firstly, mathematical backgrounds around functional data analysis and data clustering are presented. Secondly, new features that extend the geometric criteria to detect non-compliant approaches are detailed. Thirdly, the atypical approach detection method is explained. Finally, the method is illustrated on real data and specific operational situations.

II. Mathematical Backgrounds

A. Functional Data and Functional Principal Component Analysis

Functional Data Analysis considers data as functions. In aeronautics, trajectories are naturally smooth, hence the existence of the derivatives of the curves must be assumed to ensure trajectory continuity and smoothness. Trajectories are therefore usually modeled in a Hilbert space $\mathcal{H}^m$ of square integrable functions where all the derivatives until the order m are square integrable. Let $f, g \in L^2(J)$ be two functions, the inner product associated with the Hilbert space is:

$$\langle f, g \rangle = \int_J f(t)\, g(t)\, dt,$$

And the usual norm called L2-norm is consequently defined as:

$$||f||^2 = \langle f, f \rangle$$

The various FDA methods focus on the statistical analysis of a set of curves. In practice, discretizations of these functions at time t_j, $j = 1, ...m$ are observed. In aeronautics, approach trajectories map a time interval to a state space $\mathbb{R}^d$. In this paper, such curve data are discretely recorded by radar every 4 seconds. Trajectories are observed on a time interval $[0, T_i]$, which can be different for each trajectory. For this reason, the first step of FDA consists in recovering the functional nature of curve data from discretized observations by using a decomposition on a functional basis. A system of basis functions is a set of known independent functions ϕ_k. A particular property of basis functions is that every other function can be approximated with a linear combination of a sufficient number K of these basis functions. There are different basis function systems in the literature such as polynomial basis, Fourier basis, wavelet basis or smoothing spline basis [13]. In this paper, a spline basis is used. Let $\mathcal{B} = \{\phi_1, \phi_2, ...\}$ be a basis function system on a functional infinite dimension space, and X a functional variable in this space. The approximation of X of order K is:

$$\hat{X}(t) = \sum_{k=1}^{K} c_k \phi_k(t) = \mathbf{c}^{\mathrm{T}} \boldsymbol{\phi} \tag{1}$$

Where $\mathbf{c}$ is the vector of length K with the c_k coefficients, and $\boldsymbol{\phi}$ the vector of ϕ_k functions. To estimate the c_k coefficients in ϕ_k basis, the ordinary mean square method is recommended. It consists in solving the following minimization problem:

$$\underset{c_k}{\text{Min}} \quad \sum_{i=1}^{n} ||y_i - \sum_{k=1}^{K} c_k \phi_k(t_i)||^2 \tag{2}$$

Where $y_i = x(t_i)$ is the observation of a curve x at time t_i.

Usually, a smoothness regularization penalty is added to ensure the smoothness of the functions. In general, the smoothness is ensured until the order m. The penalty is therefore:

$$\int_J ||D^m \mathbf{c}^{\mathrm{T}} \boldsymbol{\phi}(s)||^2 ds \tag{3}$$

Where D^m is the order m derivative. With this modelization, the minimization problem becomes:

$$\underset{c_k}{\text{Min}} \quad \sum_{i=1}^{n} ||y_i - \sum_{k=1}^{K} c_k \phi_k(t_i)||^2 + \lambda \int_J ||D^m \mathbf{c}^{\mathrm{T}} \boldsymbol{\phi}(s)||^2 ds \tag{4}$$

Besides, FDA extends many multivariate statistical methods to the functional setting. For example, Multivariate Principal Component Analysis (MPCA) [26] was extended to functional data. MPCA is a powerful statistic method that summarizes a significant amount of data information by creating new variables as the linear combination of existent variables. It is an orthogonal projection that concentrates the majority of the data variance in the first components of the redescription space. It enables simpler representation and analysis of complex or even large dimension variables.

Let x_i, $i = 1, ..., p$ be a sampling of p statistic variables observed over n samples. A weighting vector $\boldsymbol{\xi}$ such like the redescription of x_i is f_i is defined as:

$$f_i = \sum_j \xi_j x_{ij} = \boldsymbol{\xi}^{\mathrm{T}} x_i \tag{5}$$

In practice, the redescription space is defined by using a projection on the eigenbasis space of the observations covariance matrix ordered by decreasing eigenvalues.

PCA was extended to the functional setting called Functional Principal Component Analysis (FPCA) by Deville [27] and Dauxois [28], [29]. When data are functions sampled from an underlying stochastic process, FPCA enables dimensionality reduction by estimating the Karhunen-Loève decomposition. With this decomposition, the trajectories can be represented by their decomposition coefficients on the principal component basis and considered as a small dimension vector. This process is described in Equation 6.

$$\Gamma(t) = \overline{\gamma}(t) + \sum_{j=1}^{+\infty} b_j \phi_j(t) \tag{6}$$

It consists in considering each curve Γ as the weighted sum of a mean curve $\overline{\gamma}$ plus the principal components ϕ_j by defining the orthogonal basis that maximizes the explained variance in the first dimensions. Usually, the decomposition is truncated to keep an amount of variance, which also implies dimensionality reduction. Figure 4 illustrates a very simple example. Let's consider a set of curves with a constant mean $\bar{\mu}$. These curves present only two possible variations at time t_a and t_b. The FPCA decomposition gives two principal components functions ϕ_1, ϕ_2. Each original curve can be written as a linear combination : $\bar{\mu} + b_1 \cdot \phi_1 + b_2 \cdot \phi_2$, and represented by their principal score vector (b_1, b_2).

In this paper, trajectories are not indexed with time but with the remaining trajectory distance to the runway threshold. Consistent comparisons can be obtained by using the remaining distance to the runway threshold as aircraft do not operate at the same speeds. Besides, in FPCA, the entire interval is usually studied. However, in this methodology, the whole process is applied on smaller intervals with a sliding window in order to give a local atypicality score.

B. Introduction to Machine Learning and Data Clustering

A learning process consists in using data analysis methods and artificial intelligence to predict systems behaviors. The aim is to define a model that will fit the system as best as possible

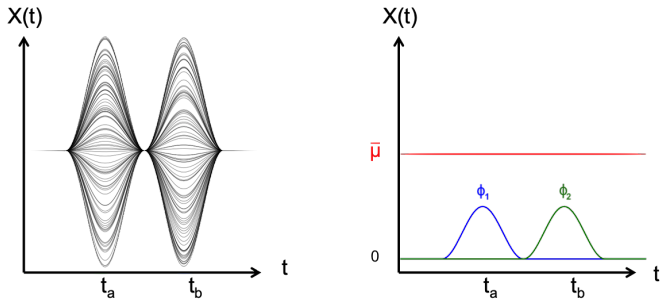


Figure 4. Illustration of a simple FPCA decomposition. On the left side are represented the original curves. On the right side, the mean and the principal component functions.

[16]. Machine learning algorithms define learning models h, that approximate the system function f:

$$f : \mathcal{X} \longrightarrow \mathcal{Y} \tag{7}$$

The function f goes from the input space $\mathcal{X}$ to the output space $\mathcal{Y}$. The input space is usually composed by defined dimension vectors of features but can also be an infinite dimension space. $\mathcal{Y}$ is a 1-dimension vector for binary classifications or unidimensional regressions. For more complex models, it is extended to a multi-dimension vector. h_θ depends on adaptive parameters θ, which are adjusted during the learning phase to fit the problem.

The learning process is applied to a finite training set $\mathcal{D}$. Unsupervised learning is characterized by training samples with only inputs of $\mathcal{X}$. Supervised learning is characterized by training samples composed of both an input of $\mathcal{X}$ and an output of $\mathcal{Y}$.

Usually, a learning algorithm tries to minimize the expected risk over θ, the adaptive parameters of h [30], [31] :

$$R(h_\theta) = \int_{\mathcal{X}\times\mathcal{Y}} l(h_\theta(X), Y)\, dP(X, Y) \tag{8}$$

Where P is the data distribution and l is a loss function, which can be defined in several ways. For regression the square loss is usually used:

$$l(h_\theta(X), Y) = (h_\theta(X) - Y)^2 \tag{9}$$

In practice, the data distribution is unknown so empirical risk replaces expected risk in the minimization problem:

$$R_{emp}(h_\theta) = \sum_{\langle X,Y\rangle \in \mathcal{D}} l(h_\theta(X), Y) \tag{10}$$

Data clustering consists in grouping similar data samples together into subsets. The inputs are unlabeled data, and the idea is to find underlying information to classify these data [16]. This property is really important. It means that no operational assumption is taken a priori, only the data structure and its statistical distribution.

A way to perform a data clustering is to solve an optimization problem that minimizes the intra-class variance and

maximizes the inter-class variance over the possible clusters. In this paper, a clustering algorithm called Hierarchical Density-Based Spatial Clustering of Applications with Noise (HDBSCAN) is used. This algorithm extends the DBSCAN clustering method [32] by converting it into a hierarchical clustering algorithm. It finally extracts a flat clustering based on the stability of clusters [33]. The algorithm is divided into five steps. It first transforms the space according to density. Secondly, it builds the minimum spanning tree of the distance weighted graph. Thirdly, a cluster hierarchy of the connected components is constructed. Then, the cluster hierarchy based on the minimum cluster size is condensed. Finally, it extracts the stable clusters from the condensed tree.

An extension to data clustering is called anomaly or outlier detection. After the clustering process, it is possible to consider as outlier the elements that fall outside the clusters, i.e. the elements that are far from any cluster. An algorithm called Global-Local Outlier Score from Hierarchies (GLOSH) gives a score between 0 and 1 for outliers [34]. It compares the density of a point to the density of any points in the associated current and child cluster. Samples with substantially lower density than the cluster density are likely to be considered as outliers.

In this paper, hierarchical clustering and outlier scoring are applied to the principal coefficients of the FPCA decomposition to compute the local atypicality coefficient.

III. Compliance Criteria Extension

In this section, the extension and the new compliance features are presented. On all the figures, colored lines are defined as follow: green is nominal, orange is a warning, red is critical. The current situation and the conformity limits for trajectories from the ELVIRA NCA module are the baselines for all the features. As such, the chevrons, the 30 second level off flight and the glide path define geometric limits.

In order to make the notion of compliance more restrictive and thereby reducing the number of false alarms, two limits are now considered: a warning limit and a critical limit. For both altitude and lateral features, the limits defined in the ELVIRA module correspond to the warning limit. Besides, a critical limit is introduced. For the altitude feature, the critical limit corresponds to the low altitude of the GIFA's 3D volumes. For the horizontal feature, the critical limit is defined as twice the warning limit. Both limits are represented in Figure 5

During approach, an aircraft is supposed to fly a levelled off flight path before intercepting the glide slope. Consequently, a new feature referred as to Glide Angle (GA) is introduced. It corresponds to the slope to join the touchdown point from the current position. Considering the earth as a sphere implies an altitude correction to compute the feature. This is illustrated in figure 6. To give an example, with 11NM distance from the runway threshold, there is an altitude difference of 107ft. The Glide Angle feature is illustrated for a trajectory in figure 7.

The warning limit and the critical limit for this feature correspond to the slope angle while intercepting Glide Slope at 4350ft and 4700ft with a nominal 4000ft FAP. The warning limit (resp. critical limit) for the Glide Angle feature is

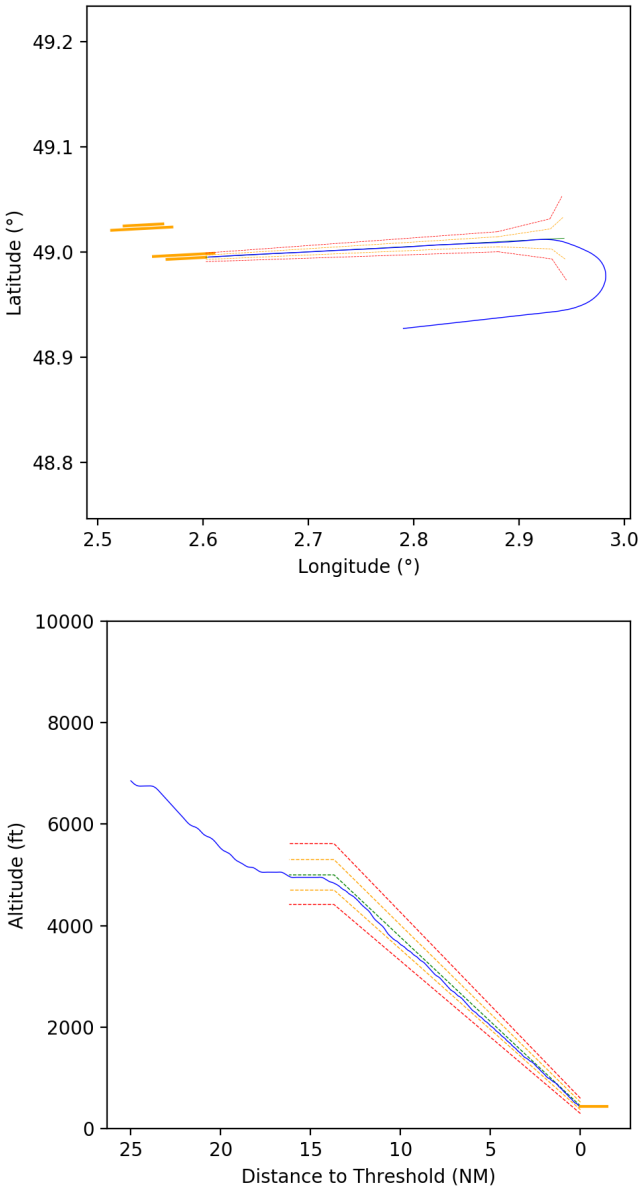


Figure 5. Extended compliance criteria of NCA module: horizontal limits (top) and vertical limits (bottom)

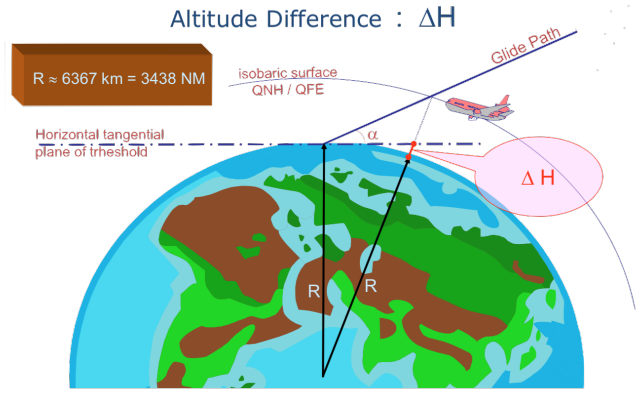


Figure 6. Illustration of altitude correction [35]

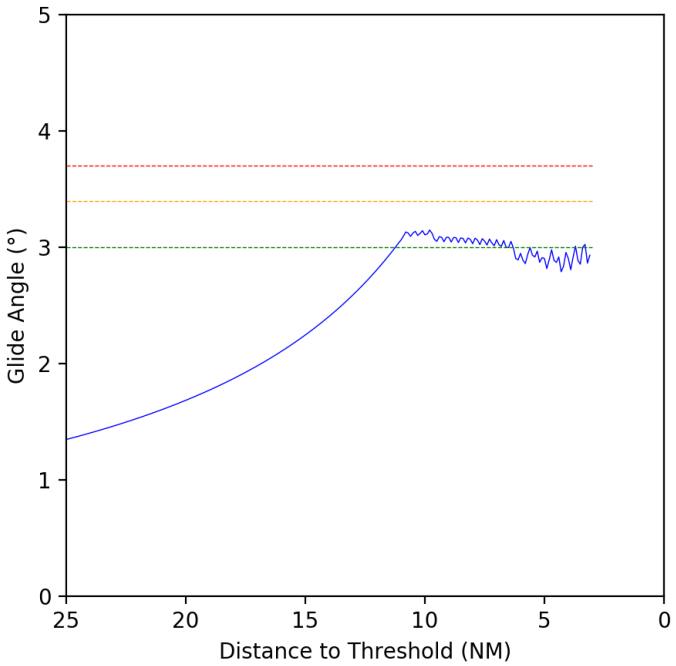


Figure 7. New criteria : glide angle. This corresponds to path angle to join runway touchdown point from current position

consequently set to 0.4° (resp. 0.7°) up to the published glide angle. This criteria starts at 25NM and ends at 3NM to avoid considering the latent fluctuation of the tangent function used to compute the feature near the touchdown point.

Finally, two other features are introduced to complete the energy analysis of the trajectories: the Ground Speed (GS) and the Vertical Speed (VS). The nominal, warning and critical limits are based on operational on-glide deceleration issues. The nominal operational on-glide deceleration in the literature is between 10 kts/NM and 20 kts/NM [36]. Consequently, a constant ground speed deceleration of 15 kts/NM from 250kts (limit speed below FL100) to the stabilization height at 1000ft with the aircraft computed approach speed v_{app} (average speed over the last 3NM) is considered as nominal. The warning limit corresponds to a 17.5 kts/NM on-glide deceleration from Chevrons to $v_{app} + 15$kts at 1000 ft and the critical limit to a 20 kts/NM deceleration from Chevrons to $v_{app} + 30$kts at 1000 ft. These limits are illustrated in Figure 8.

Regarding the vertical speed, while on glide, this is directly linked to the ground speed. Besides, we consider that before the FAP, the vertical speed is not supposed to change since the aircraft has to follow a section of levelled off flight. Finally, the warning limit (resp. critical) corresponds to a vertical speed 50% (resp. 100%) greater than the nominal vertical speed after the stabilization height.

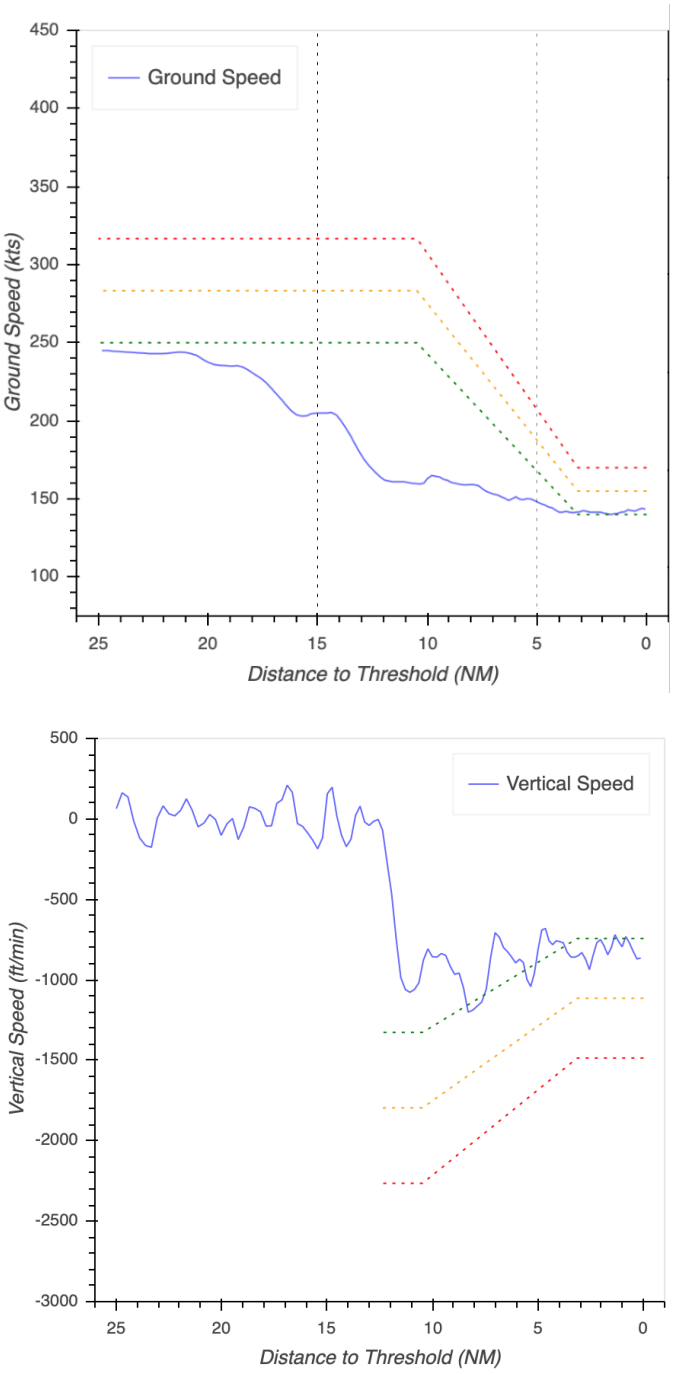


Figure 8. New criteria : ground speed (top) and vertical speed (bottom) function of the runway threshold remaining distance

IV. Atypical Flights Detection Methods

In this paper, flight data contains 3024 A320 landing radar records at CDG Airport during December 2011. The radar records are composed of longitude, latitude, altitude, ground speed, time, vertical speed, heading and aircraft type. Radar data are recorded every 4 seconds.

A. Energy Motivations

The major issue for aircraft while landing is an excess of energy. This may be found, for example, in situations where an aircraft is too high on glide slope owing to GIFA resulting in high potential energy, or has a high speed owing to tail wind in final approach or late power reduction resulting in high kinetic energy. By integrating the total energy, the tool is able to detect both cases of non-compliance.

In this study, the total energy of the aircraft is used in the runway coordinate system. Radar records do not contain aircraft mass, but since the study only concerns the last phases of flight before landing, the mass is assumed to be constant. Therefore, an approximation of the total specific energy E_T (energy per unit mass) is computed as:

$$E_T = E_c + E_p;\ E_c = \frac{1}{2} \cdot (G_s^2 + V_z^2);\ E_p = g \cdot h \qquad (11)$$

Where Ep is the specific potential energy, Ec the specific kinetic energy, G_s is the ground speed, V_z the vertical speed, h the height and g the gravity constant.

The input of the algorithms is the total specific energy as a function of the remaining distance to the runway threshold.

B. Algorithm

This method consists in applying the following process on a sliding window (defined by its width ν and its shift δ) recursively. First, a smoothing spline decomposition and an FPCA over the pieces of trajectories are applied. Then, the obtained features are projected over the k first principal components of the FPCA decomposition. Finally, a clustering to detect outliers far from every cluster is computed. The HDBSCAN algorithm was used to perform the clustering. The Global-Local Outlier Score from Hierarchies (GLOSH) is finally used to give an outlier scoring. The value given is between 0 for nominal samples and 1 for outliers. The method is summed up in algorithm 1.

Data: T: the set of specific total energy as a function of the last 25NM remaining distance to the runway threshold
Knowing the width and the shift of the sliding window, preprocess the data to obtain T_i, $i = 1...n$ subset of the energetic piece of trajectories.
for *i=1...n* **do**
  Apply Spline Decomposition on T_i subset
  Apply Functional Principal Component Analysis and keep the k first principal component coefficients
  Apply HDBSCAN clustering on the FPCA coefficient
  Return an outlier scoring of the clustering with GLOSH algorithm
end

Algorithm 1: Local Compliance Scoring by Principal Functional Component Analysis of the Total Energy Algorithm

With this algorithm, each shift of the sliding window is attributed a coefficient. To give a smoother representation of the coefficient, an averaging process is used to compute the discrete score. For example, the local compliance coefficient at 10NM is computed by averaging all the sliding window shift coefficients containing the 10NM point.

Finally, the detection phase is performed by computing the length of the maximum interval for which atypical coefficients are over a threshold τ. If the maximum interval length is greater than a reference length λ, the trajectory is considered as atypical.

C. Why is a sliding window used ?

The first question is why a sliding window is applied and why the process does not use the whole trajectory, as is usually the case in FPCA. To answer this question, the process was applied on the whole trajectory. The advantages and disadvantages of this approach are discussed below.

Radar records at CDG Airport during December 2011 were used. The study focuses on the last 15 nautical miles (18NM to 3NM from the threshold) before stabilization of A320 aircraft landing on runway 26L. First, using the whole trajectory implies only using the threshold τ to separate nominal from atypical trajectories. In this illustration, τ was fixed such that the most distant percentile of trajectories is detected. The results are illustrated in figure 9 where atypical flights are represented in red.

The detected atypical flights are analyzed using the geometric limits defined in Section III. Of the 20 flights detected, 7 were too high too high and did not respect level flight, while 9 flights demonstrated a high speed. Besides, there is a severe Glide Interception From Above shown in Figure 10. Other interesting cases can be observed. Firstly, a flight with a very large speed reduction at 9NM and with a significant lateral deviation. Secondly, a flight that intercepts the glide slope at 3000ft instead of 4000ft. Then, a flight with low speed at 5NM which sped up back to the approach speed. Finally, a landing after a go around, which therefore started with low speed at the beginning of the glide slope.

Using the whole interval presents several limitations. Firstly, τ is a data set dependent parameter defined with the data distribution. Secondly, outliers with a large score are considered as atypical. The distribution of scores obtained with this process is shown at the top of Figure 10 11. Scores near 1 are in red and scores near 0 are in green. If this distribution is compared with the labels obtained by the energetic features explained in section III, it shows that the outlier coefficient is not always appropriate since the warning and critical trajectories seem to be located on the right side of the distribution. A possible alternative could be to use a supervised learning model, applying the resulting features as labels. Then, to consider the outlier score as a function of the probability of being in the class, given by the supervised learning method. An illustration is shown at the bottom of Figure 11.

Finally, when the principal component analysis is performed over the whole trajectory, local events could have been hidden by the process. All these reasons motivate the sliding window FPCA. Furthermore, an outlier score is given for each interval, which can be interpreted as a local atypical score.

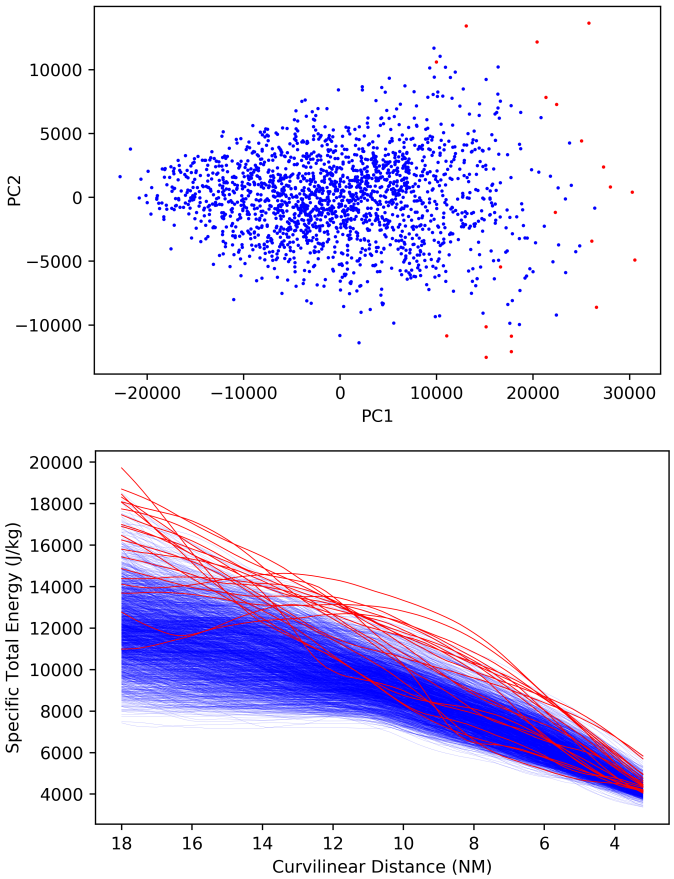


Figure 9. Projection on the two first components (Top), and representation of the total energy as a function of runway threshold remaining distance (bottom). Outliers detected are represented in red

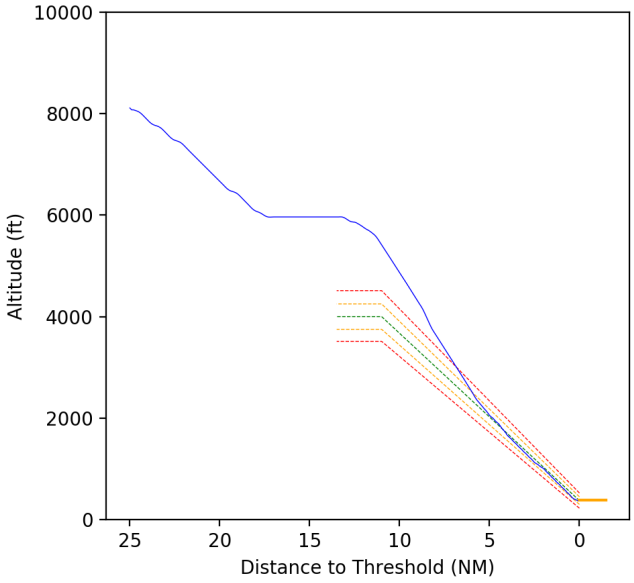


Figure 10. Glide interception from above detected as outlier by FPCA detection method

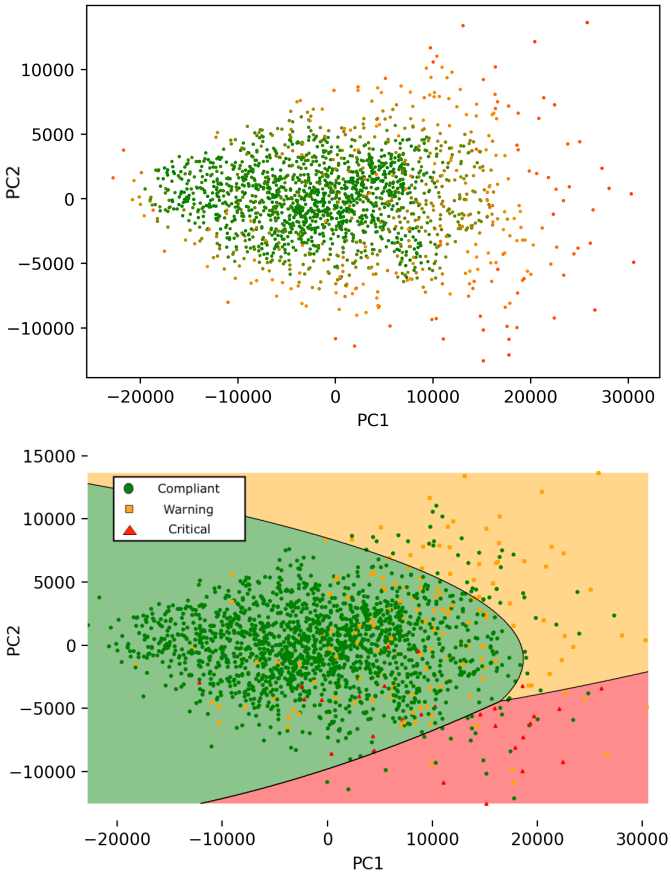


Figure 11. Representation of outlier coefficient (top) and of supervised classification with simple learning model (bottom)

D. Hyper parameters

The methodology aims at detecting atypical behaviors. Too small window slides imply a few numbers of points. Consequently, the FPCA process would not be able to capture any inherent behavior. At the opposite too large window slides would give similar results than those given in the previous section, including potential hidden local events. Different intermediate window sizes were tested (2NM, 3NM, 4NM, 5NM). They all give similar results. Therefore, the sliding window was fixed to 2NM by analogy to the operational compliance levelled-off flight of 2NM. Besides, the atypical coefficient computation uses an average of all the intervals containing the particular location. This insures a smoothness of the compliance coefficient. Finally, the detection rule parameters λ and τ should be fixed depending on what the user wants to detect. In this paper, a behavior is assumed to be atypical if it persists more than 2NM. The threshold τ was fixed statistically to categorise the highest 2% atypical trajectories.

V. Case Study Analyses

In this subsection, the results obtained for a fix configuration of the algorithm over specific situations are presented. The length of sliding window is 2NM, which corresponds to a flight of around 30s. The shift is 0.2NM (around the radar refresh time). The compliance coefficient of a point is obtained

by averaging all the coefficients over the sliding windows that contain the point. The threshold τ is fixed at 0.6 and the reference length λ to 2NM, which corresponds to the sliding window width. For the FPCA, the 3 first principal component coefficients are used. Finally, HDBSCAN uses a minimum of 10 samples per cluster. The atypical detection process was applied on the CDG approaches data set. Of the 3024 trajectories, 1.3% were considered as atypical by the algorithm. This score seems to be better proportioned than the original non-compliance criteria and implies a false alarm number reduction.

A. Continuous Descent Approach (CDA)

CDAs are situations where an aircraft operates a continuous descent and therefore does not follow a levelled off flight. The geometric limits will always notify the situation with an altitude deviation warning since the flight overpasses the altitude limits designed for levelled off flights. Nevertheless, it does not present a safety issue as it is a known procedure. The only possible issue with CDA is high energy owing to high speed. This paragraph underlines how the methodology deals with this kind of situation.

30 flights that intercepted the glide slope at an altitude above the published interception altitude and then proceeded on a CDA were selected. For all the flights that presented a nominal speed, none were considered as atypical. It suggests that the method does not detect nominal energetic behavior. Nevertheless, for those with a high ground speed such as the flight illustrated in Figure 12, which has a ground speed of around 250kts at the FAP, the sliding window detects high energy. The energy was finally dissipated but it shows that it was a potentially dangerous situation before the FAP.

Consequently, the method seems to be relevant for the study of CDA. Indeed, only approaches with high speed are considered as atypical.

a) Glide Interception From Above: In the dataset, there are 6 cases of GIFAs. The result obtained for the GIFA represented in Figure 10 are shown in Figure 13. The sliding window method is very efficient since the atypical behavior is accurately localized before 6NM. The results are similar for the 6 cases.

The method seems to be effective in the detection of significant GIFA. However, small GIFAs like bumpy profiles (flights which performed levelled off flight on glide slope to decelerate for example), resulting in an excess of potential energy, might be counterbalanced by a low ground speed. Nevertheless, this is consistent since the non-compliance induced by the excess of altitude is averaged by the low speed in an energy perspective.

B. Ground Speed Warning

In this paragraph, flights which had a ground speed warning with the geometric features are analyzed. A typical example is shown in Figure 14. The aircraft maintained a ground speed of 210 kts until 4NM and finally reduced speed, joining approach speed apparently around stabilization. For all these situations, the sliding window presents a large atypical area for the last nautical miles and flights are detected as atypical.

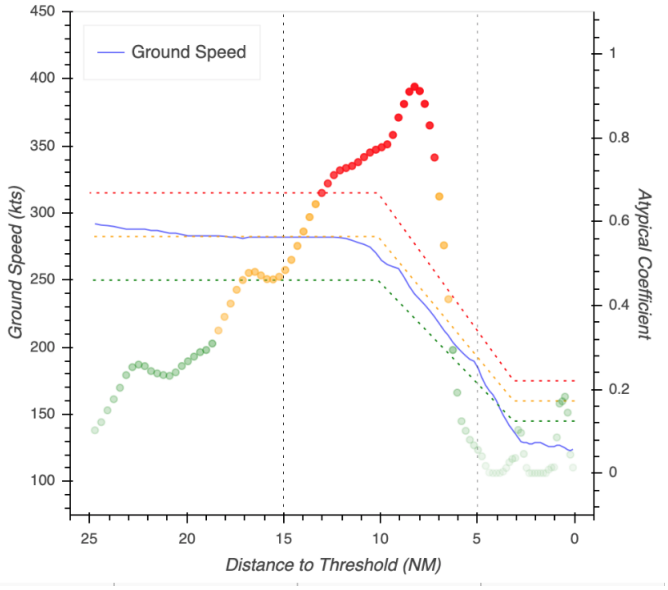


Figure 12. Ground speed and atypical coefficient of a continuous descent approach presenting high ground speed around FAP

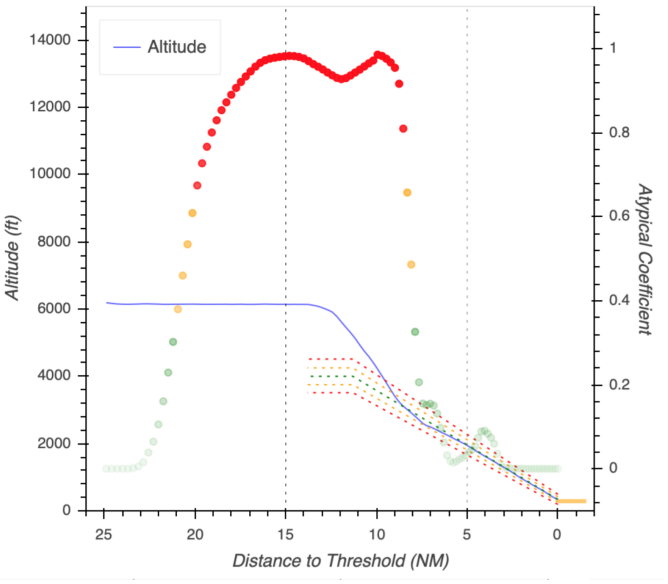


Figure 13. Sliding window energy compliance score during a GIFA

C. Nominal Flight

Finally, the nominal flights without warning are studied to be sure that they are considered as nominal by the algorithm. Over 1270 nominal flights, only 10 are considered as atypical by the algorithm. Of the 10 flights, 7 presented a low ground speed on final approach possibly owing to the wind, and 3 presented a high speed and altitude before FAP and therefore a very high total energy.

D. Methodology and result discussion

In this section, the relevance of the use of the proposed methodology is discussed.

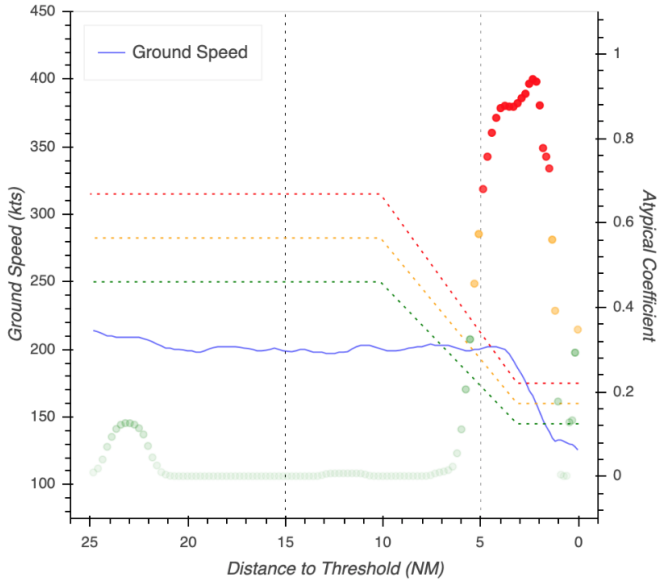


Figure 14. Ground speed and atypical coefficient of a ground speed critical flight

Firstly, as introduced in section I, national and international safety authorities would like to detect and propose appropriate corrections to undesirable events as soon as possible when they occur. The FPCA decomposition provides a possible solution since it not only takes into consideration the amplitude but also the variation of the curves. A good example is illustrated in Figure 13. Using operational criteria such as the Glide Angle would lead to a detection (altitude over-passing the 3.7° critical limit) at around 16NM. However, the proposed atypical scoring overpasses the 0.6 threshold at around 20NM and therefore starts to be atypical at 18NM considering the 2NM reference length. This is explained by the fact that other aircraft already started to reduce their energy while this aircraft kept constant potential energy. Its energy variation did not follow the group behavior and this his exactly what the methodology detects. Consequently, the first advantage of this method is that it anticipates non-nominal values considering the curve variation.

Secondly, determining safety event precursors is a complex problem. This methodology contribution is to provide potential precursors flights, considering only one assumption: atypical flights do not behave like the others. This assumption implies a dedicated analysis of the extracted flights to decide if they contain safety issues or not. Nevertheless, it has the advantage of providing flights that might not have been monitored with the current flight data analysis methods. Indeed, current safety analyses mainly focus on the stabilization phase, i.e. the last five nautical miles of the approach. To the best of the author's knowledge, only few studies have been conducted in an approach path management perspective. Underlying non-monitored behaviors enables better situation awareness. Airline safety offices or air navigation service providers could, for example, create safety advises when they consider that the behaviors present a potential threat.

VI. Conclusions

In this paper, an atypical flight detection method based on Functional Principal Component Analysis is presented. It aims at enhancing safety in the approach and landing phases of flight providing potential precursors to final events. The proposed method consists in applying a Functional Principal Component Analysis process and an outlier scoring on a sliding window. The algorithm was applied to a specific total energy profile to detect energy atypical behaviour at Charles De Gaulle airport. The results of the method were compared to geometric features built with operational limits and analyzed on typical flight approach patterns. The FPCA method accurately detects and locates different types of abnormal energy situations, and shows an interesting anticipation property.

Future works will focus on validating the methodology with on-board flight data monitoring events, and on developing a complete post-operational analysis tool based on the methodology [37]. Currently, novel data generation methods using Generative Adversarial Networks [38] is being developed. In addition, Generative Adversarial Networks enable anomaly detection and will be compared to the FPCA method. Finally, the FPCA method can be extended to develop a real-time detection tool, which could be very beneficial in the operational field.

Acknowledgment

The authors would like to give special thanks to Mr. André Vernay, Mr. Yoni Malka and Mr. Paul-Emmanuel Thurat from the French Civil Aviation Safety Authority for their significant help in understanding the operational context. The authors would also like to show their gratitude to Mr. Gaël Vincent and Mr. Brice Panel from Paris Charles-De-Gaulle Airport ATC operations for their time and their explanation of the complex Paris northern airspace and Charles-De-Gaulle approach.

References

[1] F. Jackman, "Nearly Half of Commercial Jet Accidents Occur During Final Approach, Landing," Nov. 2014.

[2] M. Tremaud, "Getting To Grips With ALAR," tech. rep., Airbus Industrie, Oct. 2000. Available at https://www.cockpitseeker.com/wp-content/uploads/goodies/ac/a320/pdf/data/GettingToGripsWithALAR.pdf.

[3] IATA, "2036 Forecast Reveals Air Passengers Will Nearly Double to 7.8 Billion," Oct. 2017. Available at https://www.iata.org/pressroom/pr/pages/2017-10-24-01.aspx.

[4] DGAC, "Safety state program, 2009-2013," 2009. Available at https://www.ecologique-solidaire.gouv.fr/sites/default/files/DGAC_Plan-Strategique_2009-2013_FR.pdf.

[5] DGAC, "Safety state program, horizon 2018," 2013. Available at https://www.ecologique-solidaire.gouv.fr/sites/default/files/DGAC-PS-2018-FR-WEB.pdf.

[6] DGAC, "Safety state program, horizon 2023," 2019. Available at https://www.ecologique-solidaire.gouv.fr/sites/default/files/DSAC_PlanHorizon_2023_FR.pdf.

[7] DGAC, "Risk portfolio, ssp 2009-2013," 2010. Available at https://www.ecologique-solidaire.gouv.fr/sites/default/files/Cartographie_Risques_10_2010.pdf.

[8] A. Vernay, "Defining a Compliant Approach (CA): A joint response to enhance the safety level of approach and landing," *HindSight17 - Safety versus Cost*, p. 44, July 2013. Available at https://www.eurocontrol.int/sites/default/files/publication/files/130704-hs17.pdf.

[9] Centro de Publicaciones, Ministerio de Fomento, "Report A-029/2011, Accident Involving a Bombardier CL-600-2b19 (CRJ200), Registration EC-ITU, Operated by Air Nostrum, at the Barcelona Airport, on 30 July 2011," tech. rep., Comisión de Investigación de Accidentes e Incidentes de Aviación Civil, Madrid, 2013. Available at https://www.fomento.gob.es/NR/rdonlyres/0E877F5B-5703-4AF3-95D9-3C6B1B8A2899/118577/2011_029_A_ENG.pdf.

[10] C. A. Hart, R. L. Sumwalt, M. R. Rosekind, and E. F. Weener, "Descent Below Visual Glidepath and Impact With Seawall Asiana Airlines Flight 214 Boeing 777-200er, HL7742 San Francisco, California July 6, 2013," tech. rep., National Transportation Safety Board, 2014. Available at https://www.ntsb.gov/investigations/AccidentReports/Reports/AAR1401.pdf.

[11] J. Ramsay and B. Silverman, *Functional Data Analysis, Second Edition*. Springer Science & Business Media, 2005.

[12] J. O. Ramsay and B. W. Silverman, *Applied Functional Data Analysis: Methods and Case Studies*. Springer, 2007.

[13] J. O. Ramsay, G. Hooker, and S. Graves, *Functional Data Analysis with R and MATLAB*. Use R!, New York: Springer-Verlag, 2009.

[14] F. Ferraty and P. Vieu, *Nonparametric Functional Data Analysis: Theory and Practice*. Springer Science & Business Media, Nov. 2006. Google-Books-ID: lMy6WPFZYFcC.

[15] F. Ferraty, *Recent Advances in Functional Data Analysis and Related Topics*. Springer Science & Business Media, June 2011. Google-Books-ID: GarlvB5ZmqwC.

[16] T. Hastie, R. Tibshirani, and J. Friedman, *The Elements of Statistical Learning: Data Mining, Inference, and Prediction*. Springer Series in Statistics, Springer New York, 2013.

[17] S. Ullah and C. F. Finch, "Applications of functional data analysis: A systematic review," *BMC Medical Research Methodology*, vol. 13, Dec. 2013.

[18] B. Gregorutti, *Forêts Aléatoires et Sélection de Variables: Analyse Des Données Des Enregistreurs de Vol Pour La Sécurité Aérienne*. PhD Thesis, Paris 6, 2015.

[19] R. Suyundykov, S. Puechmorel, and L. Ferré, "Multivariate Functional Data Clusterization by PCA in Sobolev Space Using Wavelets," in *42èmes Journées de Statistique*, 2010.

[20] C. Hurter, S. Puechmorel, F. Nicol, and A. Telea, "Functional Decomposition for Bundled Simplification of Trail Sets," *IEEE transactions on visualization and computer graphics*, vol. 24, no. 1, pp. 500–510, 2018.

[21] K. Tastambekov, *Aircraft Trajectory Prediction by Local Functional Regression*. PhD Thesis, Toulouse, INSA, 2012.

[22] F. Nicol, "Statistical Analysis of Aircraft Trajectories: a Functional Data Analysis Approach," *Alldata 2017, The Third International Conference on Big Data, Small Data, Linked Data and Open Data*, pp. pp–51, 2017.

[23] C. Barreyre, B. Laurent, J.-M. Loubes, B. Cabon, and L. Boussouf, "Multiple testing for outlier detection in functional data," *arXiv:1712.04775 [stat]*, Dec. 2017. arXiv: 1712.04775.

[24] C. Barreyre, B. Laurent, J.-M. Loubes, B. Cabon, and L. Boussouf, "Statistical Methods for Outlier Detection in Space Telemetries," in *2018 SpaceOps Conference*, (Marseille), American Institute of Aeronautics and Astronautics, May 2018.

[25] F. Yan, X. Lin, R. Li, and X. Huang, "Functional principal components analysis on moving time windows of longitudinal data: dynamic prediction of times to event," *Journal of the Royal Statistical Society: Series C (Applied Statistics)*, vol. 67, pp. 961–978, Feb. 2018.

[26] I. Jolliffe, *Principal component analysis*. Springer, 2011.

[27] J.-C. Deville, "Méthodes Statistiques et Numériques de l'analyse Harmonique," in *Annales de l'INSEE*, pp. 3–101, JSTOR, 1974.

[28] J. Dauxois, *Les Analyses Factorielles En Calcul Des Probabiblités et En Statistique: Essai d'étude Synthétique*. PhD thesis, Université Paul Sabatier, 1976.

[29] J. Dauxois, A. Pousse, and Y. Romain, "Asymptotic Theory for the Principal Component Analysis of a Vector Random Function: Some Applications to Statistical Inference," *Journal of multivariate analysis*, vol. 12, no. 1, pp. 136–154, 1982.

[30] V. Vapnik, *The Nature of Statistical Learning Theory*. Springer New York, 2013.

[31] V. Vapnik, *Statistical Learning Theory*. Adaptive and learning systems for signal processing, communications, and control, Wiley, 1998.

[32] M. Ester, H.-P. Kriegel, J. Sander, and X. Xu, "A Density-Based Algorithm for Discovering Clusters in Large Spatial Databases with Noise," *Kdd*, vol. 96, no. 34, pp. 226–231, 1996.

[33] R. J. G. B. Campello, D. Moulavi, and J. Sander, "Density-Based Clustering Based on Hierarchical Density Estimates," in *Advances in Knowledge Discovery and Data Mining*, Lecture Notes in Computer Science, pp. 160–172, Springer, Berlin, Heidelberg, Apr. 2013.

[34] R. J. G. B. Campello, D. Moulavi, A. Zimek, and J. Sander, "Hierarchical Density Estimates for Data Clustering, Visualization, and Outlier Detection," *ACM Transactions on Knowledge Discovery from Data*, vol. 10, pp. 1–51, July 2015.

[35] J.-F. Perez and S. Fournie, "Conception de procédures aux instruments - Cours IPD3f," tech. rep., École Nationale de L'Aviation Civile, 2017.

[36] C. Lemozit, "Aircraft Energy Management during Approach," tech. rep., Direction Générale de l'Aviation Civile, 2005.

[37] G. Jarry, D. Delahaye, and E. Féron, "Trajectory approach analysis: A post-operational aircraft approach analysis tool," 2019.

[38] G. Jarry, N. Couellan, and D. Delahaye, "On the use of generative adversarial networks for aircraft trajectory generation and atypical approach detection," 2019.